

Multiband Antenna for 2G/3G/4G and Sub-6 GHz 5G Applications Using Characteristic Mode Analysis

Devendra H. Patel^{1, 2, *} and Gautam D. Makwana^{3, *}

Abstract—A multi-band microstrip patch antenna consisting of an elliptical shape patch with four triangular-shaped arms mounted on a Rogers AD255C substrate with coaxial feed technique to cover 1720 MHz for 2G, 2120 MHz for 3G, 2372 MHz for 4G, and 3536 MHz for Sub-6 GHz 5G wireless communication applications is proposed in this paper. The antenna is designed by exciting a dominant & its orthogonal as well as higher order TM_{mn0}^z modes based on cavity model-circular patch theory and then reshaped to an elliptical shape to get the resonance at desired bands. A Characteristics Mode Analysis (CMA) is used for computing electromagnetic resonance frequencies in conducting bodies. A radiating characteristic of the proposed antenna structure is analyzed and verified using CMA technique for target applications frequencies. The CMA demonstrates that the proposed antenna resonates at 1728 MHz, 2127 MHz, 2358 MHz, and 3436 MHz, making them suitable for use as multi-band antenna for 2G, 3G, 4G, and Sub-6 GHz 5G applications respectively after proper feeding. A simulated bandwidth at -10 dB return loss is 23 MHz (1707–1730 MHz) for 2G, 34 MHz (2104–2138 MHz) for 3G, 18 MHz (2364–2382 MHz) for 4G, and 67 MHz (3499–3566 MHz) for Sub-6 GHz 5G applications. The simulated peak gains are 6.29 dBi, 7.08 dBi, 4.51 dBi, and 6.18 dBi which are validated by measured results at the respective resonant frequencies. An overall dimension of the proposed antenna is $100 \times 100 \times 3.175$ mm³. The proposed antenna was simulated by CST Studio Suite 2020. Measurement was done for the fabricated antenna which shows good agreement with simulated ones. The proposed multi-band antenna with low complexity and easy design offers a quasi-omnidirectional radiation pattern and performance improvement.

1. INTRODUCTION

In communication applications, microstrip patch antenna has drawn a lot of interest. In the 1970s, various theoretical analysis methods for microstrip patch antennas were conducted, including cavity techniques and transmission-line model. Currently, researchers focus more on a cavity-model approach for designing microstrip patch antennas to alleviate the shortcomings of the transmission-line model [1, 2].

Multi-band antennas have recently gained a lot of attention due to the requirements of wireless services like second-generation (2G), third-generation (3G), fourth-generation (4G), fifth-generation (5G), Worldwide Interoperability for Microwave Access (Wi-Max), Wireless Fidelity (Wi-Fi), Global Positioning System (GPS), Indian Regional Navigation Satellite System (IRNSS), etc. in a single device with reasonable impedance bandwidth and stable radiation pattern [2]. Many methods are available for designing multi-band antennas like frequency reconfigurable, fractal, metamaterial, slots, parasitic elements, etc. Because of the complexity of antennas, it is challenging for designers to define

Received 29 December 2022, Accepted 3 February 2023, Scheduled 22 February 2023

* Corresponding authors: Devendra H. Patel (pateldevendrah@gmail.com), Gautam D. Makwana (gmakwana@gmail.com).

¹ Sankalchand Patel University, Visnagar, India. ² Electronics & Communication Engineering Department, Government Engineering College, Gandhinagar, India. ³ Electronics & Communication Engineering Department, GTU — Graduate School of Engineering and Technology, Gujarat Technological University, Ahmedabad, India.

a geometrical structure for an antenna that offers a simple design, low cost, low-profile design, etc. On the other hand, constraints like gain, directivity, bandwidth, high efficiency, and desired frequency bands must be considered when designing and developing such multi-band antennas [2]. Coupling and feed-matching circuits can also support multi-band and broad-band antenna operations [3].

In this context, the present work focuses on the Theory of Characteristics Modes (TCM) which was initially developed by Garbacz and Turpin [4], later revised by Harrington and Mautz [5,6], and recently became a substitute for conventional microstrip antenna design strategy. By using the Characteristic Mode Analysis (CMA), physical insights of any structure can be examined by studying and observing the characteristics of each mode separately [4–9]. This paper attempts to develop a multi-band antenna geometrical structure for exactly predicting the resonance frequencies and field distributions using the CMA technique. CMA-based multi-band antennas have been proposed widely [7–9]. Adams et al. also presented a comprehensive review of CMA-based innovative antenna element designs including wideband, multiport, dielectric resonator, reconfigurable, and circularly polarized antennas [10]. Characteristic Modes (CM) are a class of functions that, under certain boundary conditions, diagonalize the operator that connects field and induced sources allowing it to fully describe the behavior of a studied object. They are obtained by solving a specific weighted eigenvalue equation derived from an impedance matrix using the Method of Moments (MoM). These modes are geometry-dependent and excitation independent. Later, the excitation is important, while determining the presence of particular mode(s) in geometry [4–6].

The paper is organized as follows. Section 2 provides the background theory of CMA, the proposed antenna design methodology, and its CMA analysis. The simulated and measured results are discussed in Section 3. Lastly, the work is summarized in the conclusion section.

2. CHARACTERISTIC MODE ANALYSIS (CMA) ANALYSIS AND PROPOSED ANTENNA DESIGN METHODOLOGY

2.1. Background Theory of Characteristic Mode Analysis (CMA)

The CMA technique is used in electromagnetics to solve for currents and fields generated by scattering objects of any size or material. It also provides understating of the physical phenomena of any geometric shape/form independent of any external excitation source(s) and makes its analysis, synthesis, and optimization more straightforward for any antenna designer. The resonating frequency of modes at specific application frequencies, characteristic current modes, electric field, surface current, etc. can be calculated using CMA [4–9].

The characteristic current modes and characteristic electric field (E_n) for arbitrarily shaped conducting bodies of antennas are expressed as Equations (1) and (2) respectively [4–9]:

$$J = \Sigma a_n J_n \quad (1)$$

The characteristic current (J_n) of the n^{th} characteristic mode has a unique dominating characteristic electric field (E_n) which is represented by a common coefficient (a_n) of J_n and E_n and is expressed as Equations (2) and (3) [4–9].

$$E = \Sigma a_n E_n \quad (2)$$

$$a_n = \frac{\langle E_{\text{tan}}^i(r), J_n \rangle}{1 + j\lambda_n} \quad (3)$$

where λ_n and $E_{\text{tan}}^i(r)$ represent the characteristic values in the range $(-\infty, +\infty)$, and incident tangential E -field, respectively.

The Modal Significance (MS) represents the normalized amplitude of the current modes and is defined as Equation (4). The characteristic mode at a particular frequency has the modal significant value of $MS_n = 1$ (i.e., $\lambda_n = 0$), has a high resonance, and converts into a non-radiating mode when MS_n approaches zero (i.e., $\lambda_n \rightarrow \infty$). Any conducting body has an infinite number of characteristic modes. Still, a limited number of dominant modes have high modal significant values, and the other low-value modal significance is neglected. The structure will radiate if an appropriate feed is applied in

the right location [4–9].

$$MS_n = \frac{|1|}{1+j\lambda_n} \quad (4)$$

The phase of the Characteristics Mode (CM) obtained from the Characteristics Angle (α_n) is defined as Equation (5) [4–9]:

$$\alpha_n = 180^\circ - \tan^{-1}(\lambda_n) \quad (5)$$

where α_n is the phase of n^{th} characteristics mode of conducting bodies which lie in the interval (90° , 180°). The mode is a good radiator when its characteristics angle (α_n) is 180° (i.e., $\lambda_n = 0$) or close to 180° , and the mode stores energy when the characteristics angle (α_n) is near 90° or 270° .

Another important term is λ_n in Equation (3) corresponding to the eigenvalue associated with the n^{th} characteristic mode because its magnitude indicates how well the associated mode radiates. A mode radiates more effectively when its eigenvalue (λ_n) is 0 or smaller. When $\lambda_n > 0$, the mode contributes to storing magnetic energy, and it contributes to storing electric energy when $\lambda_n < 0$ [4–9].

In the reported antenna design, the mode frequencies are first calculated using the Cavity Model-Circular Patch theory for TM_{11} & its orthogonal components, TM_{21} and TM_{31} at every mode for eigenvalue (λ_n) equal to zero. Based on this, Modal Significance and Characteristics Angle are calculated. The CMA methodology lays the way for a systematic antenna design in contrast to other antenna optimization techniques or trial-and-error procedures.

2.2. Proposed Antenna Element Design

To design multi-band characteristics needs to excite higher-order modes with dominant mode. The conventional method currently used for multi-band antenna such as cutting slots or Defected Ground Structure (DGS) on patch or ground plane increases geometry complexity and also affects the antenna performance. The presented multi-band microstrip patch antenna consisting of an elliptical shape patch with four triangular-shaped arms is designed based on a cavity model-circular patch/disc theory [1]. The reported multi-band antenna without any slots on the patch or ground offers a simple and low complexity design, broadside radiation patterns, good gain, and efficiency. The use of CMA in the reported antenna design is an optimization and analysis method for the identification of mode performances. The proposed antenna with coaxial probe feed is mounted on Rogers AD255C dielectric material of $100 \times 100 \times 3.175 \text{ mm}^3$ size with dielectric constant 2.55 and loss tangent ($\tan \delta$) < 0.002 . Figure 1 shows a step-wise evolution of the proposed antenna geometry. The CST Studio Suite 2020 is used for antenna design and simulation.

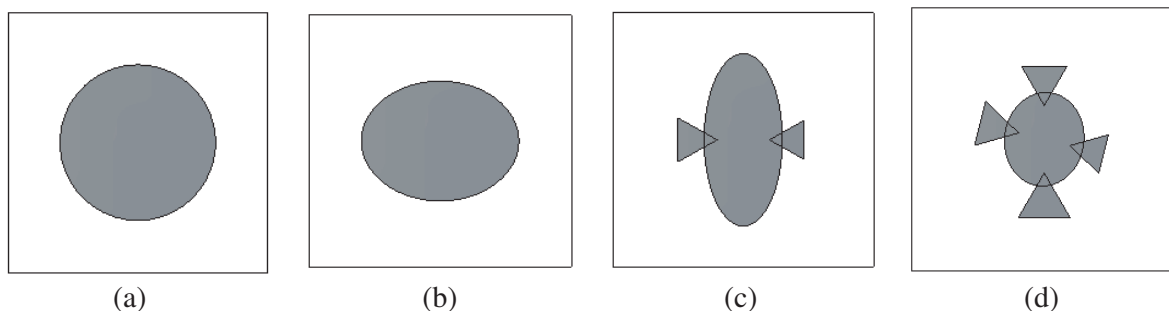


Figure 1. Evolution of Proposed Antenna Geometry Design using CMA. (a) Step-1: Single-band (1748 MHz). (b) Step-2: Dual-band (1776 and 2144 MHz). (c) Step-3: Triple-band (1616, 2125, and 2484 MHz). (d) Step-4: Quad/Multi-band (1728, 2127, 2358, and 3436 MHz)

By considering the patch, ground plane, and the material separating the two as a circular cavity, it is possible to identify the modes that the circular patch antenna supports. A circular microstrip patch antenna with a low substrate height ($h < 0.05\lambda_0$) can support the modes TM^z , where z is taken perpendicular to the patch (i.e., the fields along z are virtually constant). In the circular patch, the

modes are controlled or changed using the patch's radius, which alters each mode's absolute resonance frequency without affecting the mode's order [1].

Therefore in the cavity model, the resonant frequencies for the TM_{mn0}^z modes are found using generalized Equations (6)–(8). As a correction factor, while taking the fringing effect into account, the effective radius (a_e) in a circular patch is substituted for the actual radius (a) in Equation (6) [1].

$$(f_r)_{mn0} = \frac{1}{2\pi\sqrt{\mu\epsilon}} \left(\frac{\chi'_{mn}}{a} \right) = \frac{\chi'_{mn}\vartheta_0}{2\pi a\sqrt{\epsilon_r}} \Rightarrow (f_{rc})_{mn0} = \frac{\chi'_{mn}\vartheta_0}{2\pi a_e\sqrt{\epsilon_r}} \quad (6)$$

$$a = \frac{F}{\left\{ 1 + \frac{2h}{\pi\epsilon_r F} \left[\ln \left(\frac{\pi F}{2h} \right) + 1.7726 \right] \right\}^{1/2}}, \quad F = \frac{8.791 \times 10^9}{f_r \sqrt{\epsilon_r}}, \quad h \text{ in cm} \quad (7)$$

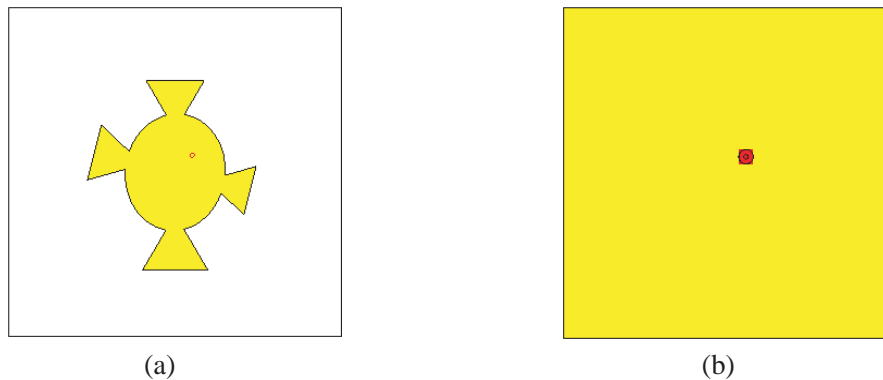
$$a_e = a \left\{ 1 + \frac{2h}{\pi a \epsilon_r} \left[\ln \left(\frac{\pi a}{2h} \right) + 1.7726 \right] \right\}^{1/2} \quad (8)$$

ϑ_0 represents the speed of light. The zeroes of the derivative of the Bessel function $J_m(x)$ are represented by the χ'_{mn} , and they establish the order of the resonant frequencies using values: $\chi'_{11} = 1.8412$, $\chi'_{21} = 3.0542$, and $\chi'_{31} = 4.2012$, and based on this values, the TM_{11}^z & its orthogonal modes, and higher order modes TM_{21}^z & TM_{31}^z are calculated.

By using a single circular or elliptical shape only the first two modes (orthogonal modes) can be adjusted, and higher-order modes cannot be controlled. Therefore, to control higher order modes extra four triangular shape arm elements with size compactness and side lengths 15.16 mm, 17.32 mm, and 19.62 mm are added and reshape the proposed antenna. These elements are chosen because of their minimal occupancy of the surface which affects the current distribution at the resonant frequencies and produces multi-band functioning. Compared to other shapes, circular, elliptical, and triangular shape elements in the antenna demonstrate better performance and can be easily analyzed with a cavity model.

The proposed design involves cavity model-circular patch associated Equations (6)–(8) in each step of Figure 1 to calculate the resonant frequency for excitation of dominant mode TM_{11} , segregated orthogonal modes, and higher order modes TM_{21} and TM_{31} contributing to the antenna radiation mechanism. Then the antenna is reshaped to an elliptical shape with triangular arms to achieve multi-band characteristics by exciting and controlling appropriate modes. The CMA is performed on step-wise design/geometry without any external excitation source(s) to validate modes and resonance for desired applications. CST Studio Suite 2020 has an in-built tool/solver into the Integral Equation Solver based on the Method of Moments (MoM) numerical method which is used to simulate and observe the characteristics modes, modal significance, eigenvalue & characteristic angle of the defined structure including the influence of dielectrics without the need for user post-processing. After validating the resonance of the proposed antenna geometry in step 4, the signal to the antenna is fed at (5.11 mm, 5.2 mm) location to examine the characteristics of the proposed antenna.

The proposed antenna is fabricated and tested in an anechoic chamber to examine its performance; pictures of it are shown in Figure 2. The return loss, Voltage Standing Wave Ratio (VSWR), gain, and radiation patterns of a fabricated antenna are measured, examined, and compared in this paper.



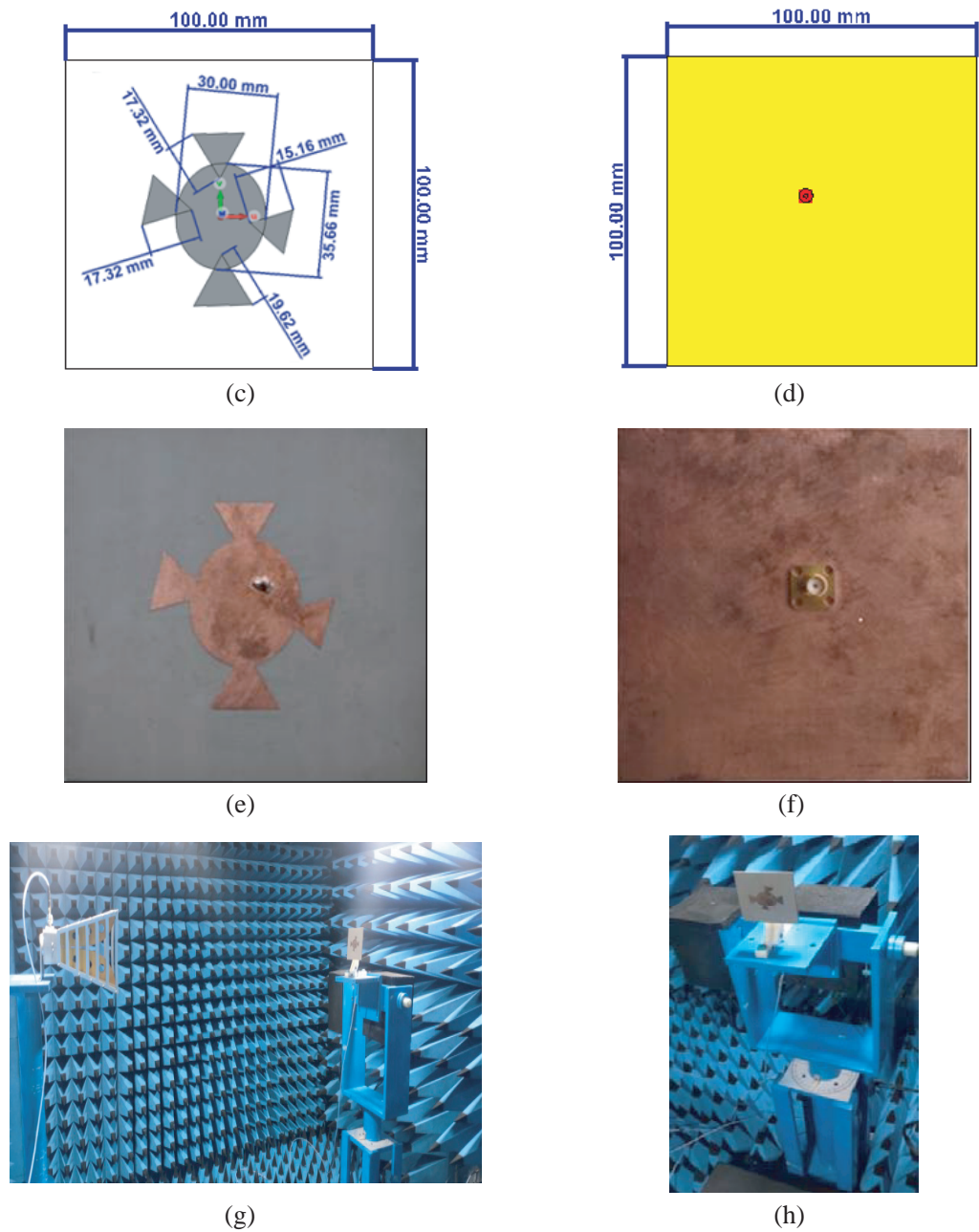


Figure 2. Proposed Antenna Design: (a) Top view. (b) Bottom view. (c)–(d) Top view & bottom view with dimensions. (e)–(f) Top view & bottom view – Fabricated. (g)–(h) Photographs of antenna parameters measurement in an anechoic chamber.

2.3. Characteristic Mode Analysis (CMA) of the Proposed Antenna

The important parameters, namely Modal Significance (MS_n), eigenvalue (λ_n), and Characteristics angle (α_n) associated with the n^{th} characteristic mode are simulated and analyzed for the proposed antenna. The MS_n value is ≈ 1 for Modes 1, 2, 4, and 5 at 1728 MHz, 2127 MHz, 2358 MHz, and 3436 MHz, respectively, for the proposed antenna showing that these modes are accountable for radiation as shown in Figure 3. Mode 3 does not emit radiation and instead stores magnetic energy ($MS_n \approx 0$, $\lambda_n > 0$). Modes 1 & 2 have eigenvalue that is nearly zero ($\lambda_n \approx 0$), and Modes 4 & 5 start with negative value

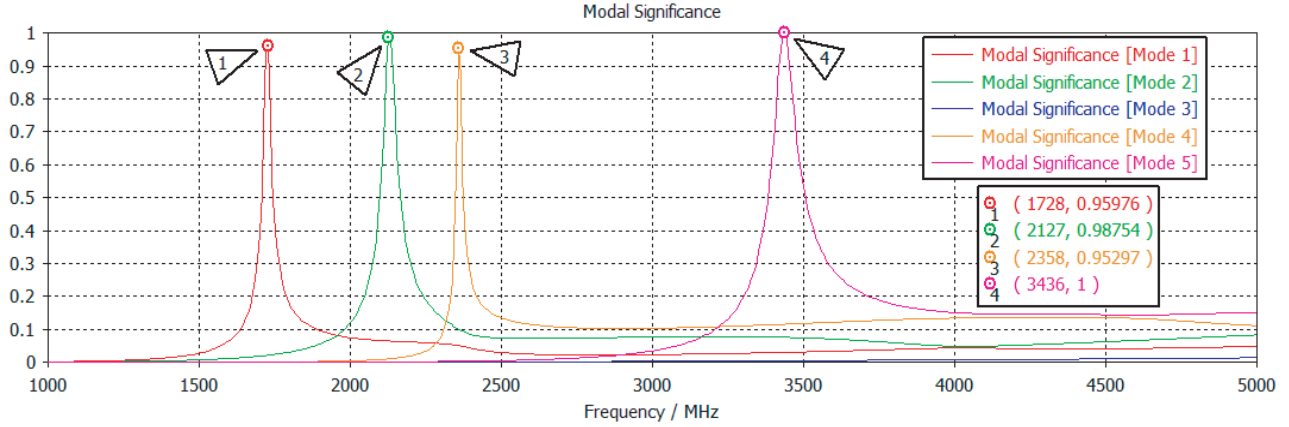


Figure 3. Modal Significance (MS_n) of a proposed antenna element.

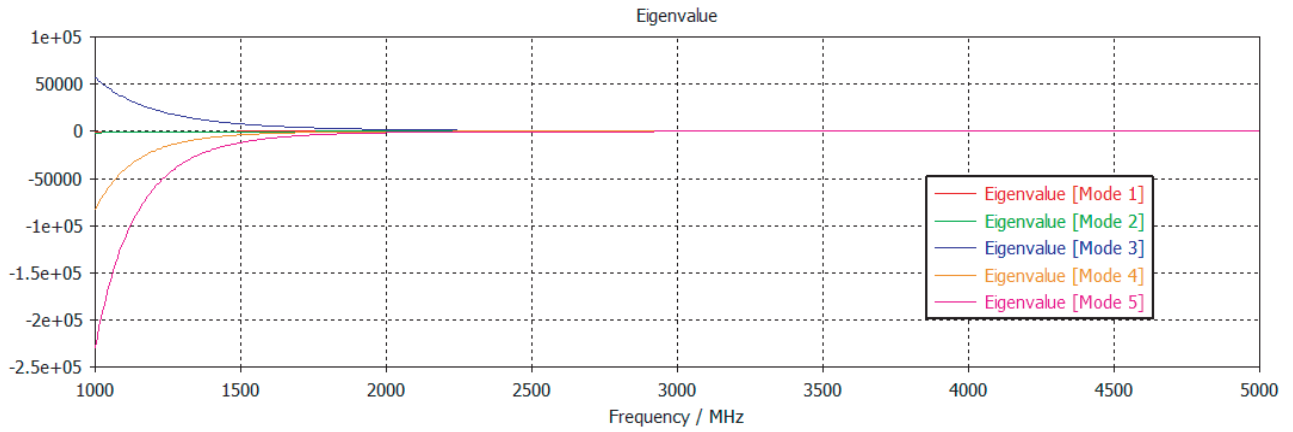


Figure 4. Eigenvalues (λ_n) of the proposed antenna.

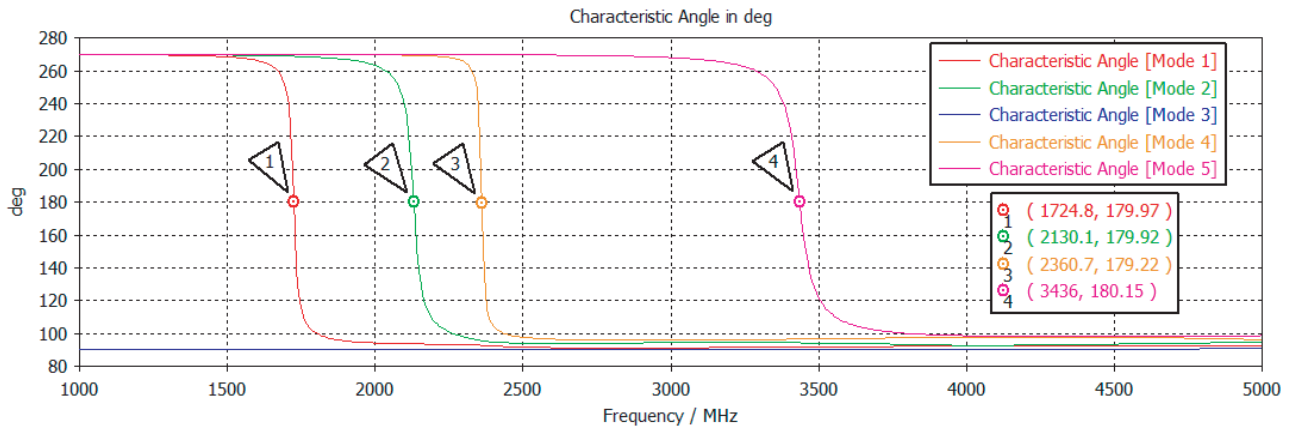


Figure 5. Characteristics Angle (α_n) of the proposed antenna.

as they store electric energy ($\lambda_n < 0$) from ~ 1000 – 2300 MHz after that eigenvalue finally keeps a small constant positive value ($\lambda_n \approx 0$) which indicates how well the associated mode radiates more effectively as shown in Figure 4. The resonance at a target frequency of each mode is easily identified by looking for the points where the characteristics angle (α_n) is $\approx 180^\circ$ (i.e., $\lambda_n \approx 0$, the mode is a good radiator) as shown in Figure 5.

The Characteristics Mode Analysis (CMA) in Figures 3–5 demonstrates that the proposed antenna with a wider patch surface is a good radiator for the target frequencies 1720 MHz, 2120 MHz, 2372 MHz, and 3536 MHz, and also offers reasonable bandwidth at each band if proper feed at a suitable location is applied. The appropriate feeding to the antenna at a particular location with the impedance of $50\ \Omega$ plays a vital role in the excitation of the antenna by suppressing certain modes and exciting the desired mode by proper feeding.

3. SIMULATED AND MEASURED RESULTS

The CST Studio Suite 2020 is used for the simulation of the various characteristics of the proposed antenna, and measurements have been made for the fabricated antenna in an anechoic chamber. The return loss and VSWR of the proposed antenna depicted in Figure 6 show that the proposed antenna covers 2G/3G/4G and Sub-6 GHz 5G applications. The simulated return loss and VSWR at 1720 MHz,

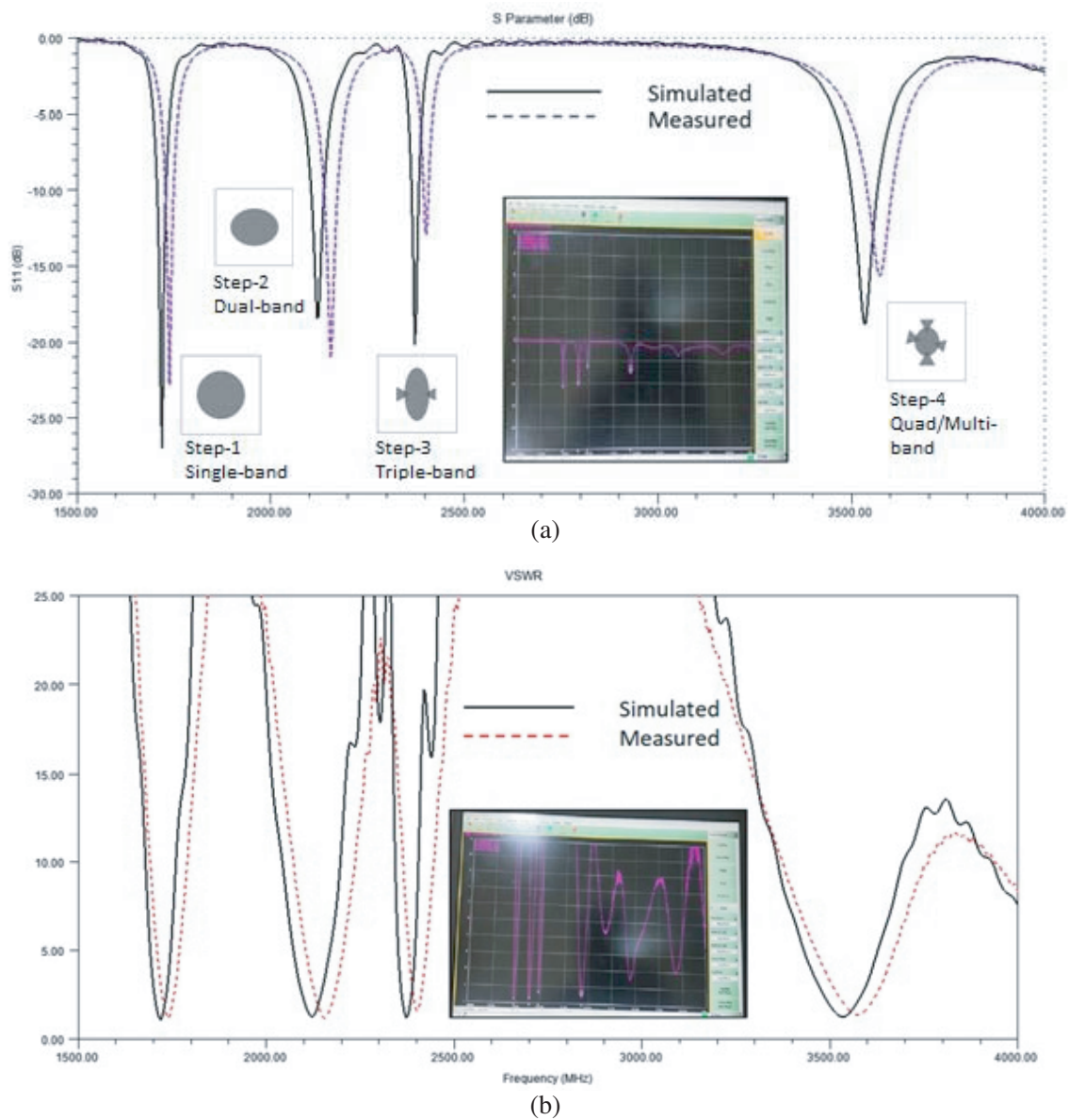


Figure 6. Simulated and Measured (a) Return Loss and (b) VSWR of the proposed antenna.

2120 MHz, 2372 MHz, and 3536 MHz are -26.83 dB, -18.44 dB, -20.12 dB, & -18.80 dB, and 1.09, 1.27, 1.22, & 1.26, respectively, which have good agreement with the measured values.

The surface current distributions at 1720 MHz, 2120 MHz, 2372 MHz, and 3536 MHz shown in Figure 7 represent the working principle of the proposed antenna. Here, the surface current distribution shows how current concentrates on the surface of the antenna structure, which results in effective radiation at a particular frequency by forming an energy loop.

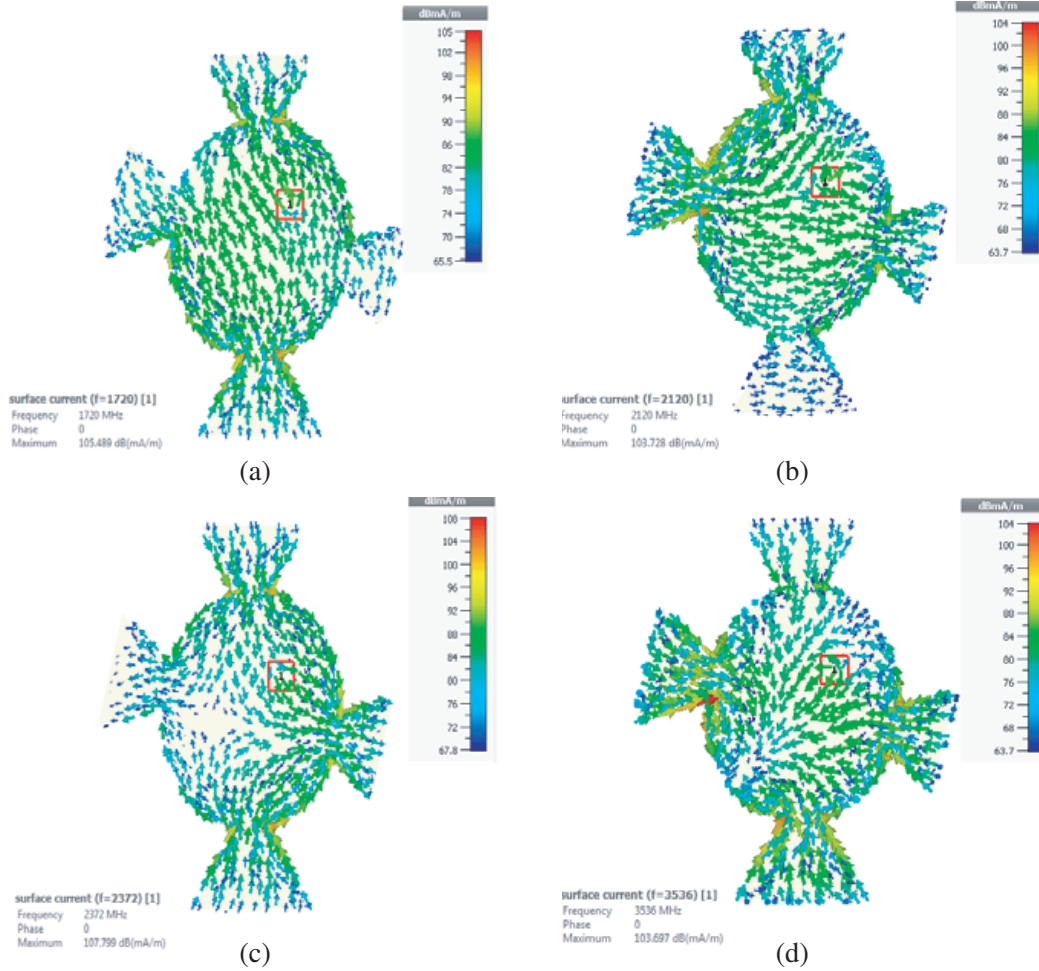


Figure 7. Surface current distributions of the proposed antenna. (a) Current distributions at 1720 MHz. (b) Current distributions at 2120 MHz. (c) Current distributions at 2372 MHz. (d) Current distributions at 3536 MHz.

The normalized far-field radiation patterns (simulated and measured) in the xz -plane (E plane, $\Phi = 0^\circ$) and xy -plane (H plane, $\Phi = 90^\circ$) are shown in Figure 8. It is seen that the proposed antenna is linearly polarized and exhibits a quasi-omnidirectional radiation pattern across the desired operating bands.

As shown in Figure 9, the measured peak gains are 5.85 dBi, 6.98 dBi, 4.24 dBi, and 5.65 dBi, demonstrate good agreement with simulated results, while the simulated radiation efficiencies are 81.9%, 92.5%, 63.3%, and 93.2% at 1720 MHz, 2120 MHz, 2372 MHz, and 3536 MHz, respectively.

The findings of the suggested antenna are well aligned between simulation and measurement. The antenna is optimized to achieve the desired application bands. It is also noted that the small discrepancy between the simulated and measured results is due to the influence of the fabrication defects, measurement environment, substrate losses, feeding network, etc. The performance comparison

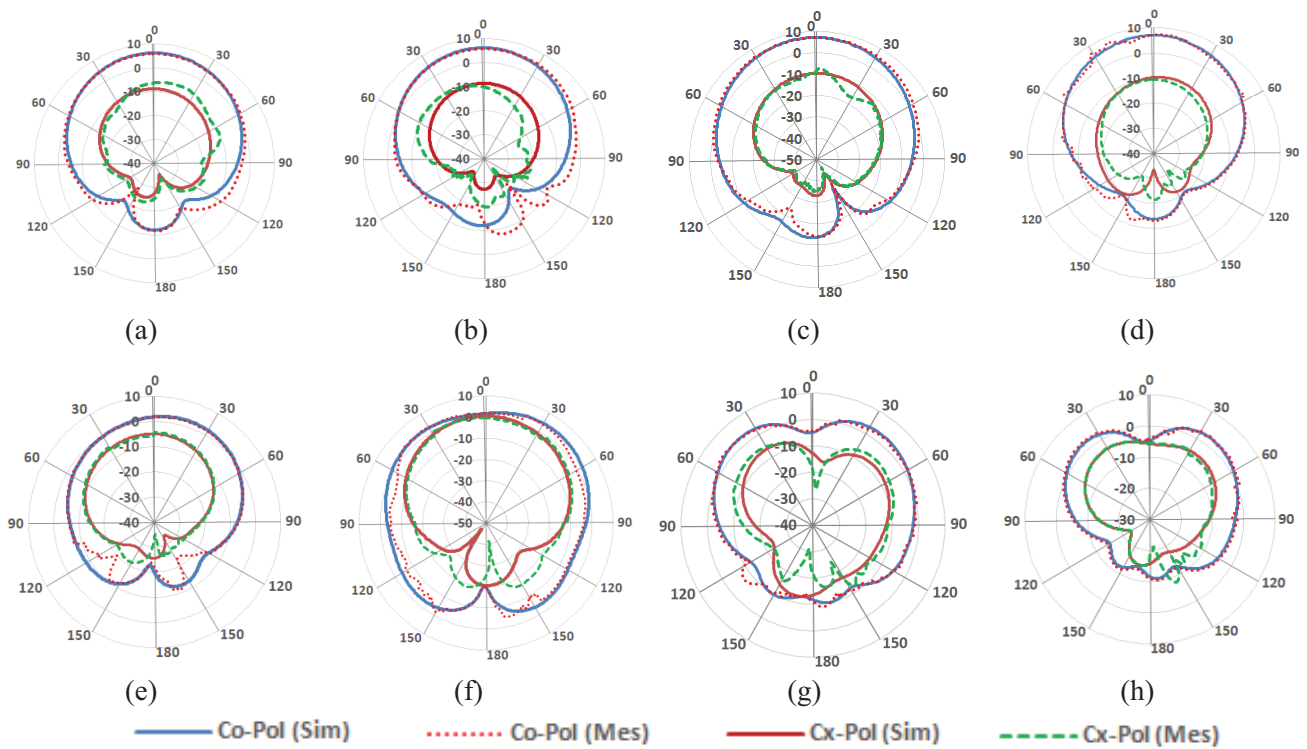


Figure 8. Simulated and measured normalized radiation patterns (co-pol and cross-pol) of the proposed antenna.

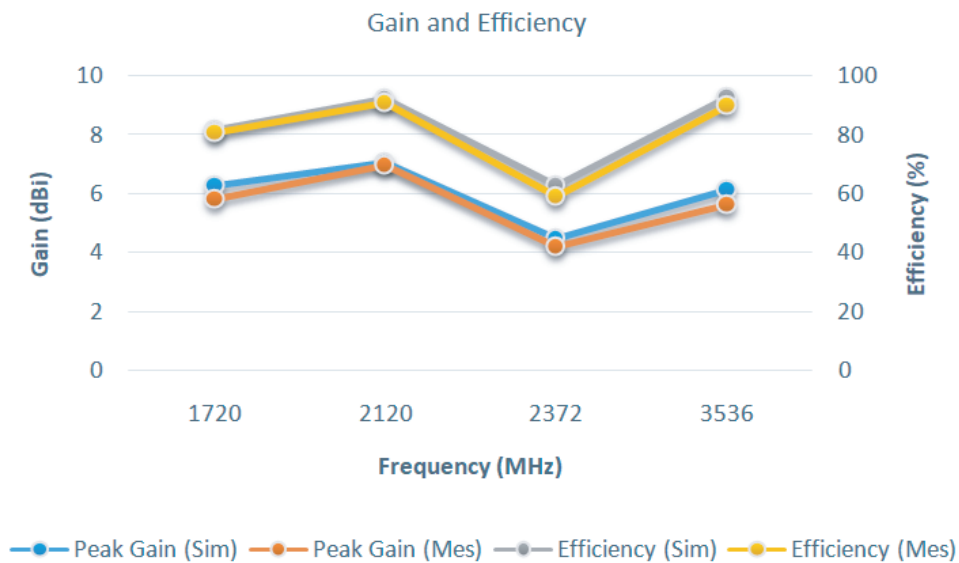


Figure 9. Simulated and Measured Gain and Efficiency of the proposed antenna.

of the proposed antenna with the reported multi-band antennas is shown in Table 1. From Table 1, it is observed that the proposed antenna has reasonable gain and efficiency and is a promising candidate for upcoming wireless communication devices.

Table 1. Proposed antenna performance comparison.

Ref.	Dimension (mm ³)	Frequency (GHz) /Applications	Method Used	Substrate	Gain (dBi)	Efficiency (~ %)	Feeding technique
[11]	120 × 65 × 1.6	2G/3G/4G /5G NR	Non-uniform planar monopole element	FR-4	4.56	-	Coaxial
[12]	0.35 × 0.35 × 0.23 (λ _L)	0.7–0.96, 1.7–2.7, 3.3–3.8	Two Dipole antennas with three Elliptical & Bowtie dipole and cat-ear-shaped arms	FR-4	5.5–8	-	Coaxial
[13]	85 × 70 × 1.6	1.6/2.35 /3.8/5.85	“回” structured monopole antenna	FR-4	0.5–5.9	10–70	Microstrip
[14]	144 × 132 × 2	2G/3G/4G	Three series fed printed strip dipoles and parasitic patch	Aluminium	4–6	-	Microstrip
[15]	88.5 × 60 × 1.6	1.6/2.6 /3.7/5.3	Monopole antenna with fractal	FR-4	1.16–3.75	40–72	CPW
[16]	50 × 45 × 1.6	0.9/1.5/2.4 /3.8/5.6/6.9	Banana leaves trapezoidal structure and four patches as leaf veins	FR-4	3.45–6.14	-	CPW
[17]	0.21 × 0.11 × 1.57 (λ _d)	1.98/2.8/3.3 /4.1/4.7/5.5	Vitis vinifera half-leaf shape and embedded arc-slits	Rogers 5880	0.2–2.66	92–99	Microstrip
[18]	97.6 × 205 × 1.6	4G/3G/2G/ WiFi/WiMAX/ WLAN/Sub-6 GHz 5G	Planar monopole antenna with inverted F-shaped and L-shaped patch/strip	FR-4	2.54–6.32	44–86	Microstrip
This work	100 × 100 × 3.175	2G/3G/4G /Sub-6 GHz 5G	Elliptical shape patch with four triangular-shaped arms	Rogers AD 255C	4.51–7.08	63–90	Coaxial

4. CONCLUSION

A multi-band microstrip patch antenna structure having an elliptical shape patch with four triangular-shaped arms fed by coaxial probe feed is proposed, and an analysis of characteristic modes is demonstrated. The proposed antenna has peak gains of 6.29 dBi, 7.08 dBi, 4.51 dBi, & 6.18 dBi, and radiation efficiencies of 81.9%, 92.5%, 63.3%, & 93.2% cover multi-band operation with impedance bandwidths of 23 MHz, 34 MHz, 18 MHz, and 67 MHz at target frequencies 1720 MHz (1707–1730 MHz), 2120 MHz (2104–2138 MHz), 2372 MHz (2364–2382 MHz), and 3536 MHz (3499–3566 MHz), respectively. The Characteristics Mode Analysis (CMA) of the proposed antenna shows a physical understanding of its current distribution and radiating behavior for multi-band operation, making it suitable for desired 2G, 3G, 4G, and Sub-6 GHz 5G applications. Using CMA, researchers optimize the antenna patch shape, size, accurate feeding placement, ground size, input impedance, current distribution concerning for the excitation of single-band or multi-band, and generation or degeneration of different modes, etc. The proposed antenna offers broadside radiation with a quasi-omnidirectional radiation pattern, appropriate gain, and radiation efficiency with a simple and low-complexity structure.

ACKNOWLEDGMENT

This research was supported in part by STI Research Project No. GUJCOST/2020-21/1262 dated 16th September 2020 of Gujarat Council on Science and Technology (GUJCOST), Gandhinagar, India. The proposed work has been tested in an anechoic chamber at the Electromagnetic and Antenna Research Centre (ELARC), Birla Vishwakarma Mahavidhyalaya, Anand, India.

REFERENCES

1. Balanis, C. A., *Antenna Theory Analysis and Design*, New Jersey Wiley, Hoboken, 2016.
2. Patel, D. H. and G. D. Makwana, "A comprehensive review on multi-band microstrip patch antenna comprising 5G wireless communication," *International Journal of Computing and Digital Systems*, Vol. 11, No. 1, 941–953, Feb. 2022.
3. Deng, J. Y., J. Yao, and L. X. Guo, "Compact multi-band antenna for mobile terminal applications," *Microwave and Optical Technology Letters*, Vol. 60, No. 7, 1691–1696, May 2018.
4. Garbacz, R. and R. Turpin, "A generalized expansion for radiated and scattered fields," *IEEE Transactions on Antennas and Propagation*, Vol. 19, No. 3, 348–358, May 1971.
5. Harrington, R. and J. Mautz, "Theory of characteristic modes for conducting bodies," *IEEE Transactions on Antennas and Propagation*, Vol. 19, No. 5, 622–628, Sep. 1971.
6. Harrington, R. and J. Mautz, "Computation of characteristic modes for conducting bodies," *IEEE Transactions on Antennas and Propagation*, Vol. 19, No. 5, 629–639, Sep. 1971.
7. Elias, B. B. Q., P. J. Soh, A. A. Al-Hadi, P. Akkaraekthalin, and G. A. E. Vandenbosch, "A review of antenna analysis using characteristic modes," *IEEE Access*, Vol. 9, 98833–98862, 2021.
8. Chen, Y. and C.-F. Wang, *Characteristic Modes: Theory and Applications in Antenna Engineering*, Wiley, Hoboken, N.J., 2016.
9. Lau, B. K., M. Capek, and A. M. Hassan, "Characteristic modes: Progress, overview, and emerging topics," *IEEE Antennas and Propagation Magazine*, Vol. 64, No. 2, 14–22, Apr. 2022.
10. Adams, J. J., S. Genovesi, B. Yang, and E. Antonino-Daviu, "Antenna element design using characteristic mode analysis: Insights and research directions," *IEEE Antennas and Propagation Magazine*, Vol. 64, No. 2, 32–40, Apr. 2022.
11. Biswas, A. and V. R. Gupta, "Multiband antenna design for smartphone covering 2G, 3G, 4G and 5G NR frequencies," *2019 3rd International Conference on Trends in Electronics and Informatics (ICOEI)*, Apr. 2019.
12. Alieldin, A., et al., "A triple-band dual-polarized indoor base station antenna for 2G, 3G, 4G and sub-6 GHz 5G applications," *IEEE Access*, Vol. 6, 49209–49216, 2018.
13. Yu, Z., Z. Lin, X. Ran, Y. Li, B. Liang, and X. Wang, "A novel '回' pane structure multiband microstrip antenna for 2G/3G/4G/5G/WLAN/navigation applications," *International Journal of Antennas and Propagation*, Vol. 2021, 1–15, Jun. 2021.
14. Zhu, X. Z., J. L. Zhang, T. Cui, and Z. Q. Zheng, "A dual-broadband printed dipole antenna for 2G/3G/4G base station applications," *International Journal of Antennas and Propagation*, Vol. 2019, Article ID 4345819, 2019.
15. Yu, Z., J. Yu, X. Ran, and C. Zhu, "A novel ancient coin-like fractal multi-band Antenna for wireless applications," *International Journal of Antennas and Propagation*, Vol. 2017, Article ID 6459286, 2017.
16. Wang, L., J. Yu, T. Xie, Z. Yu, B. Liang, and X. Xu, "The design of a multi-band bionic antenna for mobile terminals," *International Journal of RF and Microwave Computer-Aided Engineering*, Vol. 31, No. 6, 2021.
17. Abolade, J. O., D. B. O. Konditi, and V. M. Dharmadhikary, "Ultra-compact hexa-band bio-inspired antenna for 2G, 3G, 4G, and 5G wireless applications," *International Journal on Communications Antenna and Propagation (IRECAP)*, Vol. 11, No. 3, 197, Jun. 2021.
18. Azim, R., T. Alam, M. S. Mia, A. F. Almutairi, and M. T. Islam, "An octa-band planar monopole antenna for portable communication devices," *Scientific Reports*, Vol. 11, No. 1, Jul. 2021.